Innovative: International Multi-disciplinary Journal of Applied Technology
(ISSN 2995-486X) VOLUME 02 ISSUE 10, 2024

Raman Spectroscopy

Mohammad Mousa Khudair
Al-Mustansiriya University/College of Science/Department of Chemistry

Suha Salem Saadoun Saloum
Applied Chemistry/ Samarra University

Zahraa Hameed Najm
Department of Chemistry/University of Karbala/College of Science

Abbas Ayyed Kadhim
University of Al-Qadisiyah/College of Science/Department of Chemistry

Mohammed Baqir Subhan
University of Baghdad/College of Science /Department of Chemistry

Introduction

Raman spectroscopy is a technique within vibrational spectroscopy, which is based on the inelastic scattering of light. Since the development of the first commercial Raman spectrometer in 1953, advances in lasers and detectors and the discovery of new phenomena have expanded the use of this technique in several research fields [1].

Vibrational spectroscopy is related to transitions between vibrational energy levels of the molecule. It is based on one of three phenomena that occur when electromagnetic radiation interacts with a molecule: absorption, transmission and scattering. While the first two phenomena are related to middle infrared spectra (IR), the latter is the one responsible for Raman spectra [2].

The intensities of the bands in the infrared and Raman spectra depend on how effective the transfer of energy to the molecule is, and this mechanism differs between these two techniques. The condition for infrared absorption is that there is a variation in electric dipole moment of the molecule. This implies that polar bonds tend to present greater signals than nonpolar bonds. However, in Raman scattering, the activity depends on the variation of the induced dipole moment. Thus, the opposite to infrared occurs: nonpolar bonds present greater Raman signals than polar bonds. Due to this aspect, the two techniques, even while presenting signals in the same spectral range, should not be seen as duplicates of each other, but as complementary techniques. Regarding the imaging techniques using infrared and Raman, in infrared, the analysis can be much faster, while in Raman it is possible to obtain more detailed images, and lower concentrations can be more easily detected.[3]

In 1966, Delhaye and Migeon1 suggested that Raman scattering was independent of sample volume and therefore could be applied for microscopic particle analysis. From this concept, in 1974, the first Raman microspectrometers were developed and commercialized, which provided Raman point and imaging analysis. The gain obtained by combining spectral information with spatial information allowed this technique to be used to analyze various matrices, gaining prominence due to the quality of the generated results. The use of spectroscopic images allows evaluating the spatial distribution of the compounds based on their spectra, fundamental to understanding characteristics and chemical and/or physical properties related to the sample [4].

Raman imaging spectroscopy combines a microscope with a Raman spectrometer. Over the last ten years, several advances have been made and the application of Raman spectroscopy imaging has increased over the time. In some areas, it is already used as a routine technique (for example, in material characterization), while in others, it has been explored as an alternative to traditional methods (e.g., in the medical or geologic fields). Due to the diversity of applications and techniques, the aim of this review is to provide an overview of Raman spectroscopy imaging, covering its fundamentals, a brief history and applications in the last 12 years (2006-2018) [5]. The theoretical prediction of Raman scattering was made in 1923 by Smekal and experimentally proven in 1928 by researchers from two independent groups: Raman and Krishnan in India and Landsberg and Mandelstam in Russia. However, the discovery of this phenomenon was attributed only to the first group, and the effect was not only named as a tribute to Raman but he also was awarded a Nobel Prize in Physics in the year 1930 in recognition of this achievement [6]. However, the first commercial Raman spectrometer was only built in 1953, after the development of the monochromator, using mercury at a wavelength of 435.8 nm as radiation source. Thus, before the 1960’s, it was possible to identify more than 40,000 compounds using this configuration. However, the source used made the application difficult, especially for photosensitive and colored samples that intensely absorbed this radiation [7].

Thus, the invention of the laser in 1960 and its use as a light source in Raman spectrometers, being introduced by Brazilian physicist Sérgio Porto and Wood11 in 1962, presented another great advance in this type of spectroscopy, allowing its application in a faster and more reproducible manner [8].

As previously mentioned, the first suggestion of coupling a microscope to a Raman spectrometer was in 1966. However, this equipment was developed only in 1974 by Delhaye and Dhamelincourt. This new technique allowed the use of Raman spectroscopy for surface mapping. Another important step was the use of charge-coupled device (CCD) detectors from 1987. Since Raman scattering presents an inherently weak signal, this problem has been solved by using CCD detectors, improving Raman sensitivity and further extending the range of applications. Starting in the 1950’s, several variations of Raman spectroscopy were also developed, such as coherent anti-Stokes Raman spectroscopy (CARS), surface enhanced Raman spectroscopy (SERS), resonance Raman spectroscopy (RRS), tip enhanced Raman spectroscopy (TERS) and stimulated Raman spectroscopy (SRS) which brought significant improvements in several aspects (speed and/or resolution) compared to spontaneous Raman. The main events of the development of Raman spectroscopy imaging from 1920 to 2014 (in the Supplementary Information (SI) section) [9].

Raman spectroscopy presents many of the advantages of vibrational techniques, such as little or no sample preparation and direct and non-destructive analysis, considered important mainly in cases of the need for sample preservation, such as with works of arts, artefacts or forensic analysis. Another advantage is the possibility of performing analyses in the presence of water since it does not interfere with the spectra, unlike infrared spectra. Another important characteristic is that both organic and inorganic compounds present Raman signals, which allow both types to be analyzed using this technique [10].

Another advantage refers to the possibility of detecting smaller amounts of analyte compared to point spectroscopy. In point spectroscopy, one spectrum per sample, which represents the average sampled volume (often called bulk in the literature) is obtained [11]. Thus, in many cases, compounds in low concentrations are not detected. However, since in imaging spectroscopy an area of the sample is analyzed, even if the analyte is absent in several pixels, it may have a high concentration in other pixels, which allows it to be detected even at low concentrations [12].

The current energy sources of Raman spectroscopy are lasers. Monochromatic light is focused on the sample, the incident photons go into virtual state and then the scattered photons are measured. The so-called virtual state is not real and does not refer to any pre-existing electronic or vibrational state in molecule, but is created at the time of laser incidence [13].

Considering that the Raman signal strength is proportional to the fourth power of the laser wavelength, the initial impression would be that the use of more energetic lasers would provide better perfomance. However this is not always favorable since instead of the photon reaching the virtual state, it could acquire enough energy to reach the electronic excited state generating a fluorescence spectrum [14]. Therefore, aiming at improving the technique, mainly in relation to sensibility, analysis time and spatial resolution, new technologies based on the Raman scattering phenomenon were developed: SERS, CARS, TERS, SRS and RRS [15].

Resonance Raman spectroscopy (RRS), coherent anti-Stokes Raman spectroscopy (CARS) and stimulated Raman spectroscopy (SRS) RRS aims at improving the detectitvity and selectivity of Raman scattering. The Raman signal is inherently weak, but can be improved by several orders of magnitude when the wavelenght of the laser is close to the electronic absorption band that involves the resonance phenomenon. The smaller the difference between the laser frequency and the electronic transition, the stronger is the signal. However, there is a higher risk of fluorescence, and only vibrations coupled with chromophore groups are intensified. One way to prevent/ reduce fluorescence is using a laser in the ultraviolet range. A review of this technique was published in 2008 by Efremov et al., containing a brief history and the main applications [16].

Although the cited techniques present better spatial resolution and/or sensibility, they are usually slow. The issue of speed becomes crucial especially in in vivo studies. In this sense, two nonlinear Raman techniques (i.e., when the signal intensity does not depende linearly on excitation intensity) can be highlighted: CARS and SRS. Both are considered ultra-fast (around 10-15 to 10-6 s per spectrum) and present good sensibility (10-6 mol L-1). Since at room temperature most electrons are at the fundamental energy level, anti-Stokes scattering is very weak in relation to all the other Raman scattering phenomena [17].

The Raman experiment:

The theory of Raman spectroscopy and the effect of light on matter are explained. Further, the general setup for Raman spectroscopy is shown including its extension to Spectro electrochemical measurements. Gamry's measurement software and data evaluation are explained based on Spectro electrochemical experiments [18].

Raman spectroscopy is a widely used spectroscopic method. Highly specific spectra of materials can be obtained which can be compared and identified by using spectral databases. Similar to IR-spectroscopy, fundamental vibrations of molecules are examined which is important for a complete understanding of chemical reactions [19].

However, in contrast to IR-spectroscopy, no absorption effects are observed but scattering of light. As water is a strong absorber, Raman spectroscopy is the method of choice for studying aqueous solutions compared to IR-spectroscopy. This makes it suitable for biological and medical research, e.g. analysis of the impact of drugs on biological cells [20].

Raman spectra can be acquired very fast. Hence it is used for a large variety of in-situ analyses. Further, it is in general a non-destructive technique depending on the intensity of the laser and duration of an experiment [21].

The experimental setup is simple as no sample preparation is necessary. Solid or liquid samples can be used as they are received. Experiments can be performed either inside or outside of a measurement cell through glass or plastic [22].

When light is focused on matter, both interact in different ways with each other. Light can be absorbed, scattered, transmitted, or reflected amongst other effects which would go beyond the scope of this discussion [23,24].

In 1828, the Indian physicist Sir C. V. Raman performed a series of measurements where he focused sunlight on a liquid probe (see Figure 1) [25].

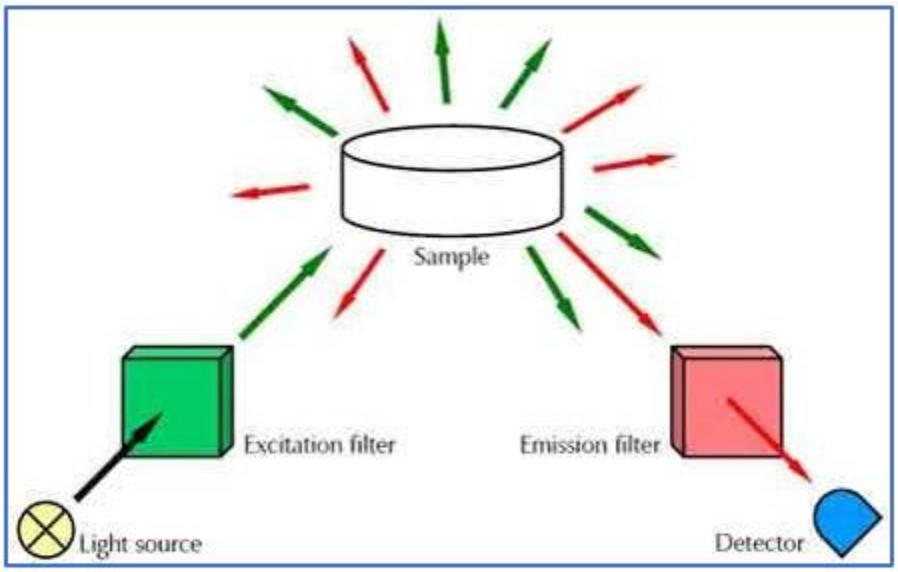

Figure 1: Simplified setup of a Raman experiment

He used a monochromatic filter (excitation filter) which let only light with a specific wavelength reach the probe. The measured scattered light showed a broader spectrum with additional wavelengths. A second filter (emission filter) behind the probe allowed blocking the incident wavelength. The observed residual scattered light could now be clearly distinguished from the incident light [26].

Light scattering

The observations which Sir Raman made can be explained by the fact that photons which are not absorbed by the probe will be scattered.[27]

In UV-Vis absorption spectroscopy, electrons in the ground state are excited to a so-called excited electronic state. For this, the photon energy (depending on the wavelength) has to match the difference in the energy states. As a result, those absorbed wavelengths cannot be found in the transmitting light.[28]

When light is scattered, electrons are also excited from their ground state. However, the photon energy is does not have to be resonant. Molecules can be excited to a virtual energy state, (see Figure 2)[29].

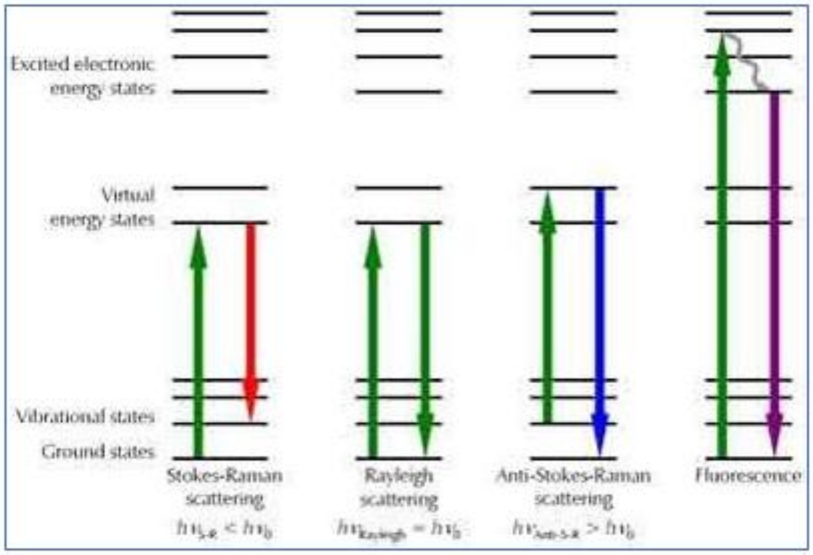

Figure 2: Jablonski diagram showing transition of energy for

Rayleigh and Raman scattering

Scattered light itself can be distinguished between elastic and inelastic scattering. The major part scatters elastic which means that the energy (i.e. wavelength) of the incident light is equal to the emitted light. This phenomenon is referred to as Rayleigh scattering [30].

Only a minor part scatters inelastically where a small fraction of energy is transferred between molecule and photon. It causes changes in the polarization of the molecule which are induced by molecular vibrations. Hence energy and wavelength of incident and scattered light are not equal anymore. This effect was observed by Sir Raman in his experiments which were described in the previous section. As a result, this kind of spectroscopy is called Raman spectroscopy.

Inelastic scattering can be further distinguished between two different forms, depending on the energy state of the molecule (see Figure 2). In case one, the molecule is initially in its ground state. After excitation, the molecule falls back to a vibrational energy state above the ground state. As a result, the emitted photon has less energy than before and the scattered light will shift to a higher wavelength. This effect is called Stokes-Raman-scattering [31,32].

The second type of inelastic scattering assumes that the molecule is already in a higher vibrational state. After excitation, the photon falls back to the molecule's ground state. The emitted photon has a higher energy than before.

The wavelength shifts to lower values. This effect is called Anti-Stokes-Raman scattering.

Anti-Stokes-Raman scattering is mostly weaker than Stokes-Raman scattering as most molecules are initially in their ground state. Hence Stokes-Raman scattering is mainly measured in Raman spectroscopy [33].

Measurement setup

Figure 3 shows a general setup for spectroscopic and Spectro electrochemical Raman experiments. It consists of a Raman spectrometer, measurement cell, potentiostat, and computer [34].

The light source of a Raman spectrometer is in general a laser with a specific wavelength. The laser's wavelength can range from the Ultraviolet to the visible and near-Infrared range depending on the application [35].

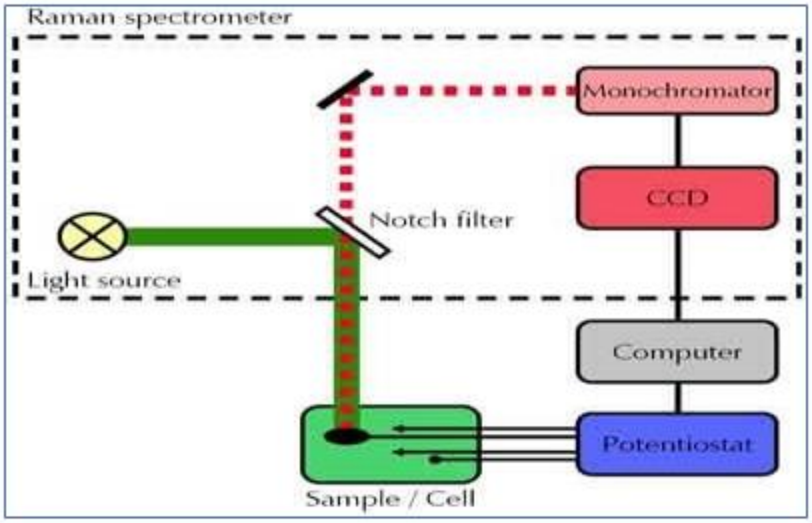

Figure 3: Experimental setup for spectroelectrochemical Raman experiments.

The light beam is focused on a dichroic filter (Notch filter). The filter reflects the light beam to the sample at a right angle. The resulting Raman scattering is focused back to the dichroic filter. It serves as band-stop filter whereby the incident light from the light source is nearly completely attenuated. Only light with a different wavelength, i.e. Raman scattered light, can pass the filter unaltered [36].

The measured light is redirected by mirrors to a monochromator which uses grating to diffract the beam into a narrow band of wavelengths. The photo current from each wavelength section is then measured at the detector. In general, a CCD detector (charged-coupled device) is used to the measured photo current into electric current. Finally, the measured data can be saved and evaluated on a computer by using appropriate software [37].

For spectroelectrochemical measurements, the target sample is used as working electrode. Reference and counter electrode complete the electrochemical cell. All electrodes are connected to a potentiostat which is also connected to a computer. Using appropriate software enables simultaneous recording of spectroscopic and electrochemical data and subsequent data evaluation [38].

Applications:

Raman imaging spectroscopy has seen increasing interest in several areas. A total of 1785 published articles were found, with the number increasing over time. In this research, we did not consider articles that used an image spectrometer only to make point measurements, i.e., without interest in the spatial distribution/chemical image [39].We also found 123 review articles or perspectives on Raman spectroscopy imaging, whether referring to the technique and advances in general or its application in a given area. Regarding the application areas, main areas were found: agriculture/biomass, environmental, biological and medical analysis, development of methods or instruments, pharmaceutical applications, geological analysis/planet and celestial bodies composition, food, arts, archaeology, material characterization, forensic analysis and archaeology [40]. The area with the largest number of published articles in the 12 years studied is material characterization, followed by biological and drug analysis. The others represent less than 10% of the total each one. Spontaneous Raman is the most used in these studies (76% of the total), followed by SERS, which represents 10%. CARS and TERS account for 4% each. The other techniques each represent a percentage below 2% of the total [41].

Agriculture and biomass

The articles on the application of Raman spectroscopy imaging in the area of agriculture and biomass during the studied period can be divided mainly into the analysis of pesticides and their effects, characterization of seeds, fertilizers and soils, studies of agricultural products, and the characterization of plant cell walls for the production of biofuel from lignocellulosic materials. In the majority of cases, the Raman image was not used alone, but associated with other imaging techniques, such as SEM, TEM and AFM or with chromatographic techniques (mainly high-performance liquid chromatography, HPLC) for the characterization of samples; there were few cases where Raman was used alone [42].

There is a predominance of the use of univariate methods (71%) and the use of spontaneous Raman (73%) for treatment and data acquisition, respectively. SERS (19%), resonant Raman (4%) and SORS (4%) techniques were found as Raman variations. The SORS method is relatively recent, developed in 2005. It uses spontaneous Raman, but obtains spectra from the internal part of the sample without the need to open/destroy the sample. Its potential has been exploited in seed characterization since normally these samples must be cut to obtain the infrared and Raman spectra from its internal part. With the use of SORS, this procedure was avoided and the methodology proved to be non-destructive for this type of sample [43].

Biofuel production has attracted attention in recent years, but lignocellulosic materials, the most abundant in nature, present low yields for bioethanol production. One of the main reasons for this problem is the cell walls, which protect plants from external attacks. This resistance is not only a product of the quantities of compounds, but also of their spatial distribution. Therefore, Raman imaging spectroscopy has been applied, aiming at this characterization, before and after the treatments for the destruction of cell walls, trying to find which pretreatment is the most effective, or even trying to understand the mechanisms of the process [44].

Foodstuff

In the area of foodstuffs, publications were found both for the characterization of products and for studies of pesticides presence and adulteration processes. Different from the other areas, there was a slightly greater predominance of multivariate methods (44%) than univariate methods (39%), with a significant percentage using both methods (17%). There is a great predominance in the use of spontaneous Raman (83%), followed by SERS (11%) and SORS (6%) [45].

Wang et al. used SERS for the detection of bacteria in skimmed milk. Using this method, it was possible to construct maps and identify the presence of the species of Salmonella enterica, Escherichia coli BL21, Listeria monocytogenes 18 and Lactococcus lactis bacteria. This type of analysis is of great importance in the area of food since Salmonella is a known food pathogen and the second largest agent responsible for human gastrointestinal infections. Zhang et al. used MCRALS on Raman and mid-infrared images to construct maps of constituent distributions in white chocolate and milk. It was possible not only to identify sucrose, lactose, fat and whey, but also an unknown compound. From the maps obtained it was possible to locate the butter and whey scattered and trapped around the sugar particles. The other constituents were distributed in heterogeneously separated particulates [46].

Recently, Yaseen et al. published a review on the use of Raman images for quality control and food safety evaluation, citing recent studies involving the technique, as well as future perspectives for application in industry and research in this sector [47].

Environmental

Articles from the environmental area represent only 2% of the total number of papers, mostly focused on the effects of pollution on the environment. It is a promising area due to both the current concern with the environment and to the possibilities found, since it is an area little explored by

Raman spectroscopy imaging to now. The form of data treatment is predominantly univariate (71%) and the acquisition is mostly from spontaneous Raman (93%) [48].

Käppler et al. used IR and Raman imaging to study environmental microplastics. This material is a contaminant of aquatic ecosystems, with negative impacts on biota. The authors showed that in cases of very colorful materials, the use of both techniques can be advantageous because many fillings and pigments have Raman spectrum, but not IR. However, the use of only Raman microspectroscopy can lead to errors, especially for painted particles. The authors' results allowed distinguishing microplastics in relation to number, type and size, as well as measurement time. Batonneau et al. analyzed urban tropospheric aerosol particles using confocal Raman allied with MCR. The results were compared to X-ray mapping and were compatible [49]. Particles rich in lead and zinc metals mixed with mineral dust were detected in the Northeast of the city when the wind was coming from the Western sector. The authors believe that these particles were possibly suspended in the troposphere by the action of wind or mechanical disturbance of polluted soils [50].

Biological and medical

This area has the second highest number of applications. It is mainly divided into two parts: studies/characterizations of cells (vegetable, animal or human) and studies of diseases, in which efforts for the diagnosis and identification of cancer cells can be highlighted. The term label-free was found mainly in these applications, highlighting the use of a dye free method, such as the traditional methods of microscopy. It was the area with the greatest diversity of Raman techniques, although spontaneous Raman still represents 68% of the articles found. In many cases, the traditional method of diagnosis is histopathological analysis. This method is subjective and requires an experienced analyst. Therefore, the development of methods that are more objective in their results is highly desirable [50].

Studies on spatial changes and with the time of cytochemistry in colonies of human embryonic steam cells were performed by Konorov et al. This allowed a better understanding of the niches of these colonies and aspects of the tissue, morphologies and organ trajectories. Han et al. studied the metabolism of antitumor drug 6-mercaptopurine in living cells. Using SERS, the authors could visualize the real-time distribuition of drug and its biotransformation in tumor cells. Marini et al. detected stretched DNA using microRaman spectroscopy and superhydrophobic substrate [51]. This work showed that this technique can distinguish DNA molecules due to chemical conformation behaviour and can be used in several applications on bio-medical field, as interaction with toxins or proteins. Using the advantage of high spatial, sensivity and velocity of SRS, Saar et al. presented an in vivo video-rate molecular imaging in mice, humans of the drug penetration of topically applied drugs. In summary, Raman imaging has been used for a wide variety of matrices in biological applications: teeth, tissues, cells, monitoring of drugs in cells and their biotransformations, bacteria, biological pathways, in vivo or in vitro analysis, among others. The need for the analysis of these highly different matrices justifies the use of different variations of Raman spectroscopy (SRS, CARS, TERS, RR and SERS, for example) [52]. Some problems are found in this type of study using the Raman image, and one of the most relevant is the analysis time. It is not uncommon for image aquisition to take several hours, which would make in vivo use difficult. Attempting to reduce time would affect image resolution, which in many cases is not desirable. An alternative is the use of other methods besides spontaneous Raman; CARS and SRS are the most used in this application since they are fast and do not need sample preparation. The use of SERS for locating particles in specific parts/organs is also an important area of research in recent years, with in vivo studies being carried out in small animals, such as mice. There is also the problem of fluorescence in this type of sample, making its application even more difficult, which is partially solved by the use of lower energy lasers, in spite of the loss in sensibility. There are several reviews on the application of Raman spectroscopy imaging in the literature for biological and medical applications. Those made by Krafft et al. (use of linear and non-linear Raman imaging of cells and tissues) and by Jermyn et al. (advances in the area with emphasis on transference for clinical analysis, mainly in cancer treatment) should be higlighted [53].

Development of equipment and methods

Raman spectroscopy imaging is not a consolidated area yet, and there is much to be investigated, either to improve the performance of the method or the equipment. Duarte et al.,79 for example, developed CARS microscope with Fourier transform for imaging. Using this equipment, it was possible to obtain an image of the entire region at the same time, decreasing the damage to the sample [54].Modifications in the TERS tips are also found, aiming at improving the performance of the method, the techniques to improve data (e.g., removal of spikes or improving signal to noise ratio), the development of SORS for linear mapping, and others. It is possible to find articles that try to develop new equipment or do modifications for new applications and/or performance improvements, as well as new modes of data processing. Most of these articles on equipment are not found in the area of chemistry, but in articles focused on the areas of physics and engineering, dealing with the optics, such as Microelectronic Engineering, Applied Physics Letters, Optics Communications and Optics Letters, among others. The variants SRS, CARS, TERS and SERS, being more recent techniques, are the ones that appear more often in this area, with more prominence for the non-linear techniques CARS and SRS [54].

Forensic analysis

The book 'Introduction to Química Forense' defines forensic chemistry as: "the part of chemistry that deals with forensic investigation in the field of specialized chemistry in order to meet aspects of judicial interest". The main applications in this area using Raman spectroscopy imaging refer to studies of fingerprints, explosives, adulterations and fraud in documents. However, many of the studies on adulteration have been included in other areas depending on the matrix analyzed (mainly drugs and food) [55].

Fingerprint detection is important in both identification and explosivecontaminated fingerprint situations. This is due to the fact that fingerprints are unique to each individual, and therefore important forensic evidence. Using a solution of β-carotene and oil, Deng et al. obtained Raman spectroscopy images of fingerprints from volunteers on several types of surfaces. A good match was obtained with the real fingerprint, independent of the surface. Document frauds are mainly identified either by distinguishing different types of ink or by the order in which the writing was performed. Borba et al. used MCR-ALS to find the order of the traces of some writing and also concealment of writing. This was possible using confocal Raman because it allows the acquisition of data at different depths. An example using a stand-off method was provided in the detection of explosives. In this method, both the analyst and the equipment were at a certain distance from the sample, and the data could be collected without approximation. In this case, pentaerythritol tetranitrate (PETN) and ammonium nitrate (NH_4NO_3) were analyzed at low concentrations, with the limit of detection estimated at ca. 1 μg cm^{-2}. The stand-off analysis of explosives brings safety to the operator [56].

Pharmaceutics

Raman imaging spectroscopy is an important analytical tool in the pharmaceutical industry, being used in both the development and in the quality control of drugs. The spatial distribution of the compounds in a sample may be associated with their effects and with the stability of the product. Different processing methods and their effects, studies of impurities, adulterations, among others are also evaluated. Scoutaris et al. studied the effect of different formulation processes on the distribution of paracetamol and found that more homogeneous formulations were obtained in pre-mixed extruded formulations than those extruded by the method of hot fusion or obtained by direct compression of the drug with the excipients [57].

The Raman imaging has also attracted attention in the study of different polymorphic forms of drugs since it is more sensitive than IR and near infrared (NIR) spectroscopies to the crystallinity and polymorphism of compounds. The study of polymorphism is particularly important in the pharmaceutical field as it is directly linked to formulation stability and safety. Piqueras et al. have developed a work to monitor the polymorphic transformations of carbamazepine, an antiepileptic approved worldwide and considered an essential drug by the World Health Organization (WHO). This method has allowed the detection of polymorphic forms I and III. The two forms are the most common forms of carbamazepine, with form III as the main form used in drug products, while form I is found at higher temperatures. These results can help to determine the storage conditions and optimization of the drug product manufacturing processes.26 Not only active pharmacecutical ingredients can present structural changes over the time but also the excipients, as in case of semi-solid formulations. Mitsutake et al. described structural changes in polyethylene-glycol/polysorbate 80 mixtures over time by different chemometric methods [58].

Interpretation of Raman spectra:

The results of a Raman spectroscopy analysis are usually represented graphically, with the intensity of the scattered light (y-axis) plotted against the frequency of light (x-axis). Also considered an indication of energy, frequency is usually measured by a unit known as the wavenumber, which is represented as reciprocal centimetres (cm^{-1}). Frequencies are plotted in relation to that of the laser, since the change in energy of the light is of interest.

A light beam is made up of many waves of light, each with different frequencies all propagating along the same path. Each frequency plays a part in the total intensity of the beam (I), which is represented as photons per time interval. The strength of a light beam is the value that is ultimately assessed with a spectrometer, with the intensity distribution of all detected frequencies known as the beam's spectrum [58].

Raman Spectroscopy of Organic and Inorganic Molecules

The Raman spectrum (especially for organic molecules) is usually considered to be composed of three distinct regions.

- The region called “fingerprint” (600-1800 cm^{-1})
- The region called “silent” (1800-2800 cm^{-1})
- The region of high wavenumbers (2800-3800 cm^{-1})

Each of these regions of the Raman spectrum contains peaks with different chemical and biochemical information, and together they can provide a lot of information about the underlying chemistry. The **position** of a Raman peak provides information on that particular chemical bond. For bonds that are found only in a particular class of molecules or that are particularly abundant in a class of molecules, the presence of a peak at a given Raman shift could indicate the presence of those molecules in the test sample. The **intensity** of a Raman peak is related to the concentration of a particular chemical bond (and therefore potentially also to the concentration of a particular class of molecules). By comparing the normalized Raman spectra of two different samples acquired on the same system, the relative heights of the Raman peaks can be used to do a relative quantification of the different molecules present [58].

- “Fingerprint” Region

In most biological applications of Raman spectroscopy, fingerprint regions provide the greatest wealth of biochemical information. Here we can find peaks that correspond to information on nucleic acids, proteins and lipids, thus providing information on both the composition and the state of the cell or tissue under examination [59]. **“Silent” Region**

The "silent" region separates the "fingerprint" region from the high wavenumbers region of the Raman spectrum and is named after the fact that no endogenous biomolecule shows peaks in this region [59].

➢ High wavenumber region

The high wavenumbers region consists of two main peaks: the peak centered at ~2900 cm^{-1} occurs for the stretching modes of the CH, CH_2 and CH_3 groups and therefore contains information on the presence of these chemical bonds, while the main peak at ~3400 cm^{-1} occurs due to the stretching mode of the OH bond and thus provides information on the water content of the substance [59].

Survey of some compounds

1- Acetone

Acetone is the simplest ketone. Its chemical formula is CH_3-CO-CH_3; the carbon atom to which the oxygen atom is bonded has *sp*^{2} hybridization and is located in the center of a triangle (approximately equilateral) whose vertices are made up of the oxygen atom and the other two carbon atoms. The CCC angle is a little less than 120°. Acetone is a mobile, colorless, volatile and flammable liquid with a characteristic ethereal odor; it is completely soluble in water, ethanol and ether and is mainly used as a general purpose solvent. In Fig. 4, we report the Raman spectrum of the molecule. The emission maxima corresponding to the modes of vibration, *stretching* and *bending* of the C-H bond of the methyl group CH_3, and of the C-C and C-O bonds are evident.

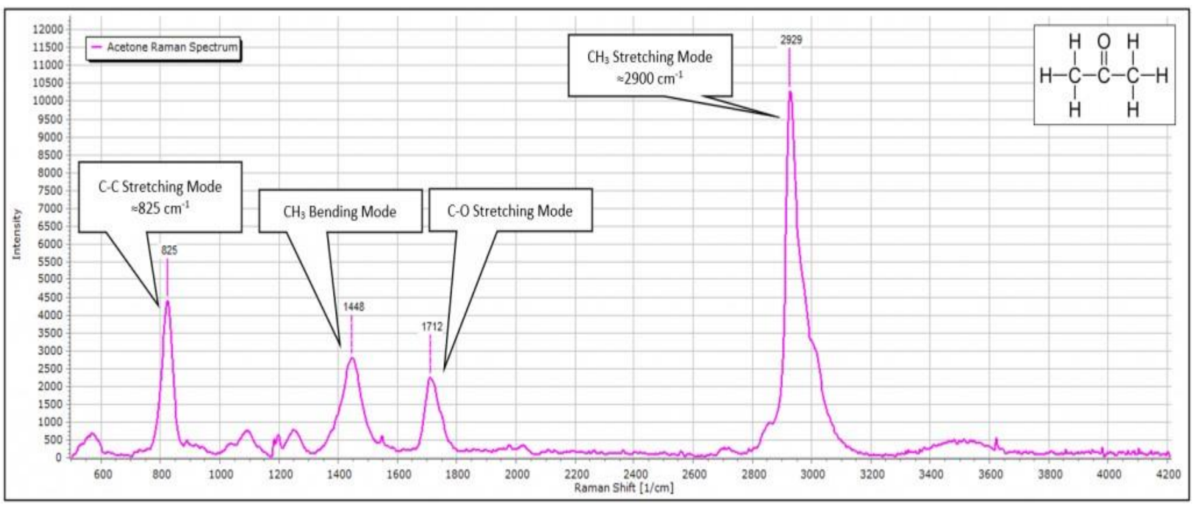

Fig 4: Raman spectrum of Acetone

2- Acetic acid

Acetic acid is an organic chemical compound whose chemical formula is CH_3COOH, best known for giving vinegar its characteristic acrid taste and pungent odor. In Fig. 5, we report the Raman spectrum of the molecule and the comparison with the Raman spectrum of acetone. The emission maxima corresponding to the modes of vibration, *stretching* and *bending* of the C-H bond of the methyl group CH_3, and of the C-C and C-O bonds are evident. We note how the emission lines substantially coincide with the exception of the one corresponding to the C-C bond, this difference is due to the difference in the overall structure of the two molecules [60].

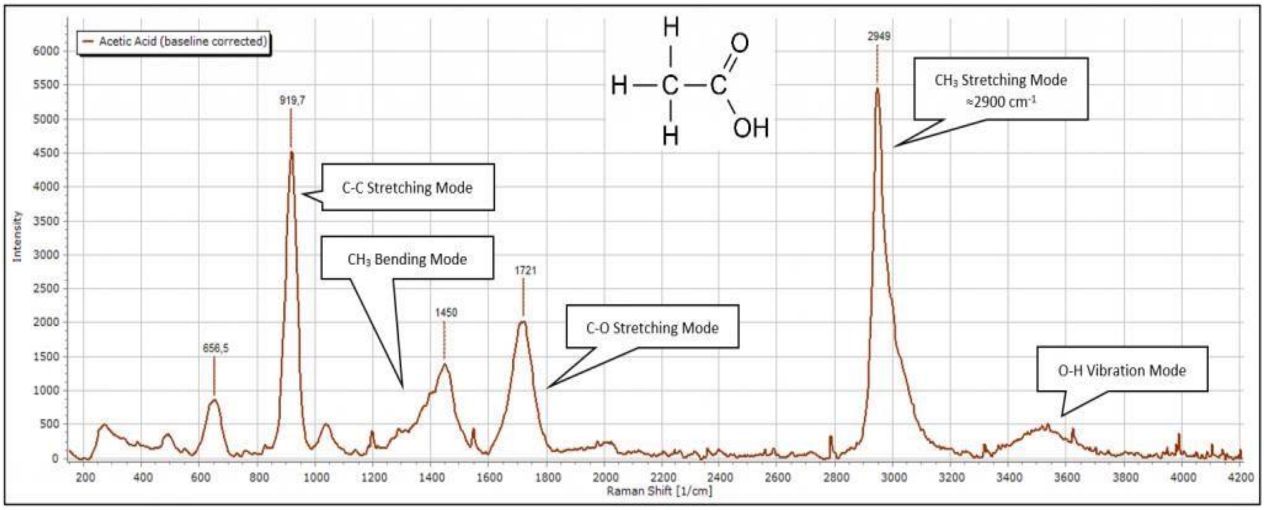

Fig 5: Raman spectrum of Acetic acid

3- Toluene

This aromatic chemical compound, consisting of a **benzene ring** to which a **methyl group** is bonded, used as a solvent and as an ingredient in gasoline and some explosives. In Fig. 6, we report the Raman spectrum of the molecule. In the spectrum we note the presence of the line at 2900 cm^{-1} which corresponds to the *stretching* vibration mode of the methyl group CH_3. At about 3000 cm^{-1} there is the stretching mode due to the bond between the methyl group and the benzene ring. Between 200 cm^{-1} and 1600 cm^{-1} there are the maximum emissions due to the vibrations of the benzene ring. The peak is also visible at about 200 cm^{-1}, near the minimum limit of the instrument.[60]

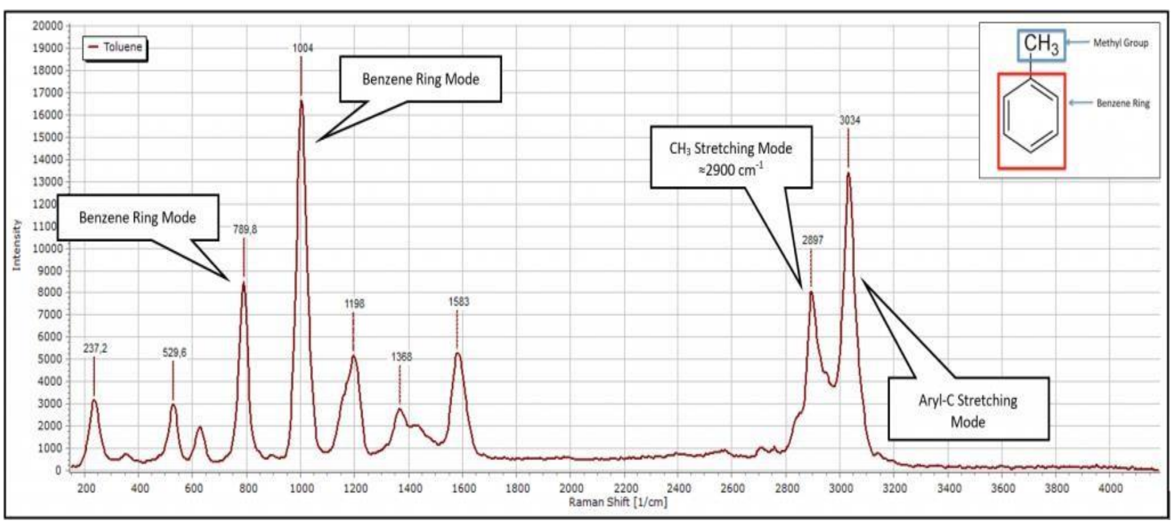

Fig 6: Raman spectrum of Toluene

4- Nitric acid

Nitric acid is a strong mineral acid as well as a strong oxidizing agent. Liquid at room temperature, colorless when very pure (light yellow otherwise); its chemical formula is HNO_3, sometimes also rendered as $NO_2(OH)$. Its salts are called nitrates and are almost all soluble in water. In concentrated solution (> 68%) it is called fuming, due to the tendency to release reddish vapors of nitrogen dioxide (NO_2). In Fig. 7, we report the Raman spectrum of nitric acid obtained with our spectrometer. We note the presence of the maxima corresponding to the vibration frequencies of the molecular groups NO_3, NO_2, and of the N-OH and N-O-N bonds [60].

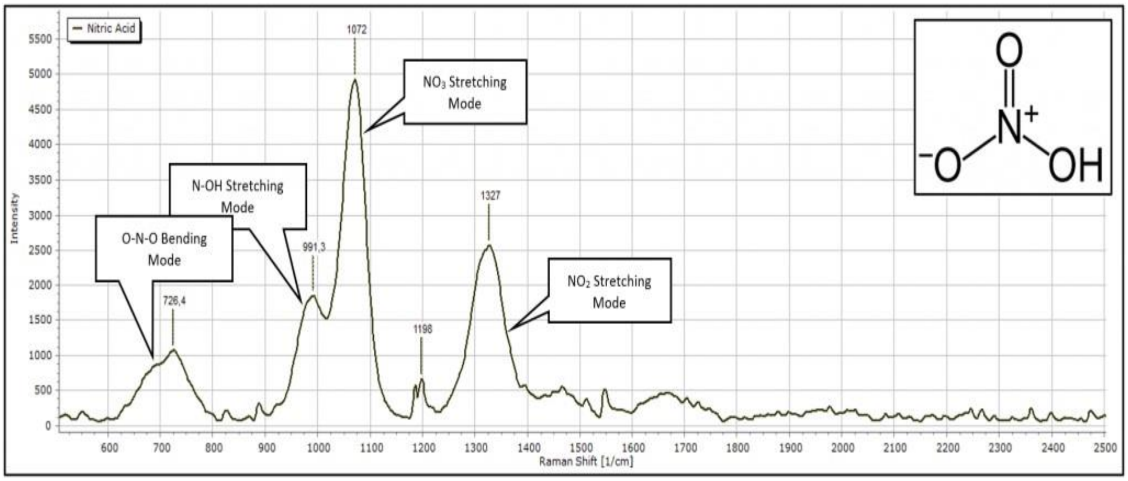

Fig 7: Raman spectrum of Nitric acid 5- Urea

Urea is a chemical compound with the formula $CO(NH_2)_2$; under normal conditions it appears as a colorless crystalline solid; it is the diamide of carbonic acid. The urea molecule is planar in the crystalline structure, while it assumes a pyramidal shape in the gas phase. In the solid state, each oxygen is bonded to two other molecules with a hydrogen bond. Given its ability to form hydrogen bonds, urea is highly soluble in water and can form clathrates by trapping numerous organic compounds. In Fig. 8, we report the Raman spectrum of an aqueous solution of urea. The peaks corresponding to the vibration modes of the NH_2 molecular group and of the N-C-N bond are present [61].

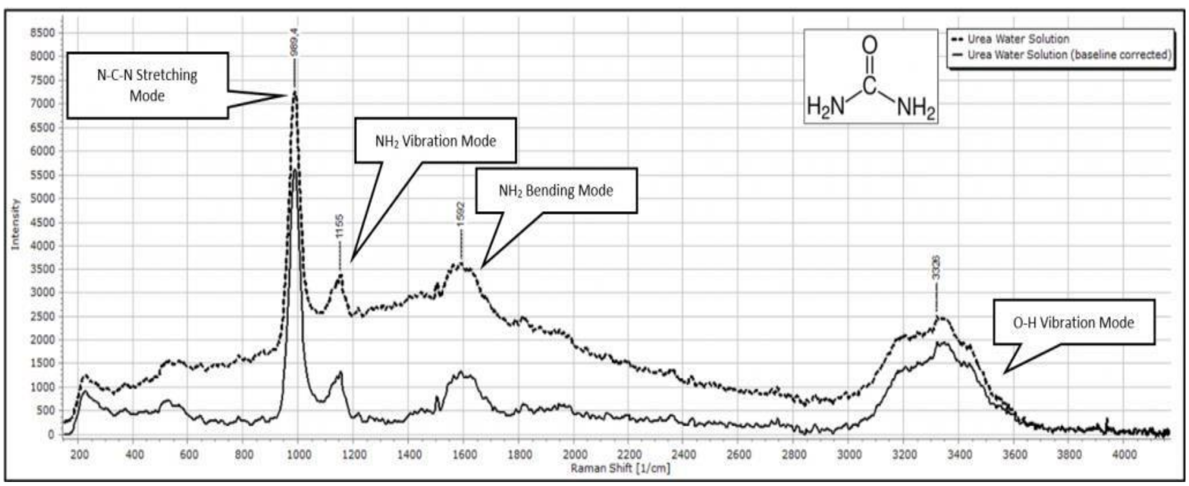

Fig 8: Raman spectrum of urea

6- Dimethyl Sulfoxide (DMSO)

Dimethyl sulfoxide (**DMSO**) is an organic compound belonging to the category of sulfoxides. At room temperature it appears as a colorless and odorless liquid that is particularly hygroscopic. DMSO is an aprotic solvent, miscible with a wide range of solvents, including alcohols, ethers, ketones, chlorinated and aromatics. It is also miscible in all proportions with water. In Fig. 8, we report the Raman spectrum, in which we note the characteristic maxima corresponding to the bonds with the sulfur atom and the methyl group CH_3. As for the silicon of the siloxanes, also in this case, due to the greater mass of the sulfur atom, the frequencies are lower than those characteristic of the bonds with carbon.

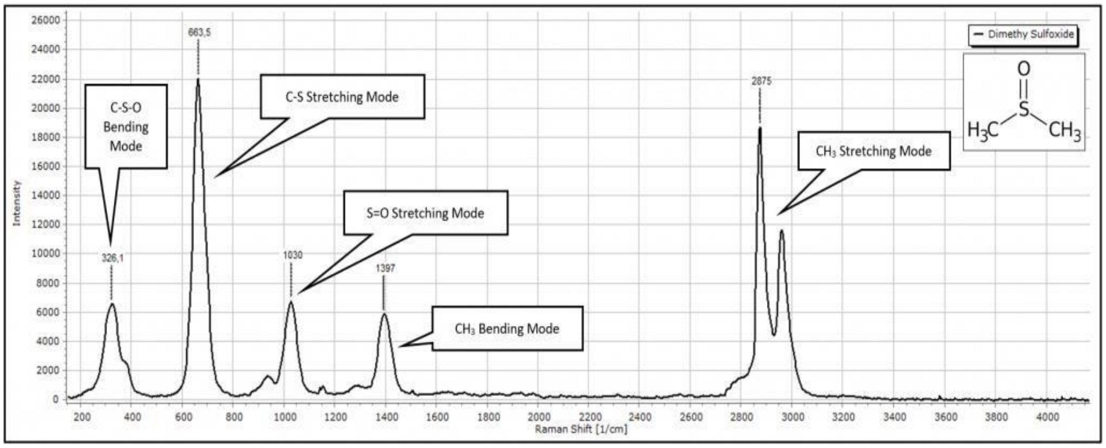

Fig 8: Raman spectrum of Dimethyl Sulfoxide

7- Dichloromethane

Dichloromethane (also abbreviated to **DCM**) is a chemical compound widely used as a solvent for organic chemistry. Its structure is similar of methane, but with two chlorine atoms that replace two hydrogen atoms. At room temperature it appears as a colorless and volatile liquid with a sweet smell. In Fig. 9, we report the Raman spectrum with the evidence of the maxima due to the C-H and C-Cl bonds. As for the silicon of siloxanes, also in this case, due to the greater mass of the chlorine atom, the frequencies are lower than those characteristic of the bonds with carbon [61].

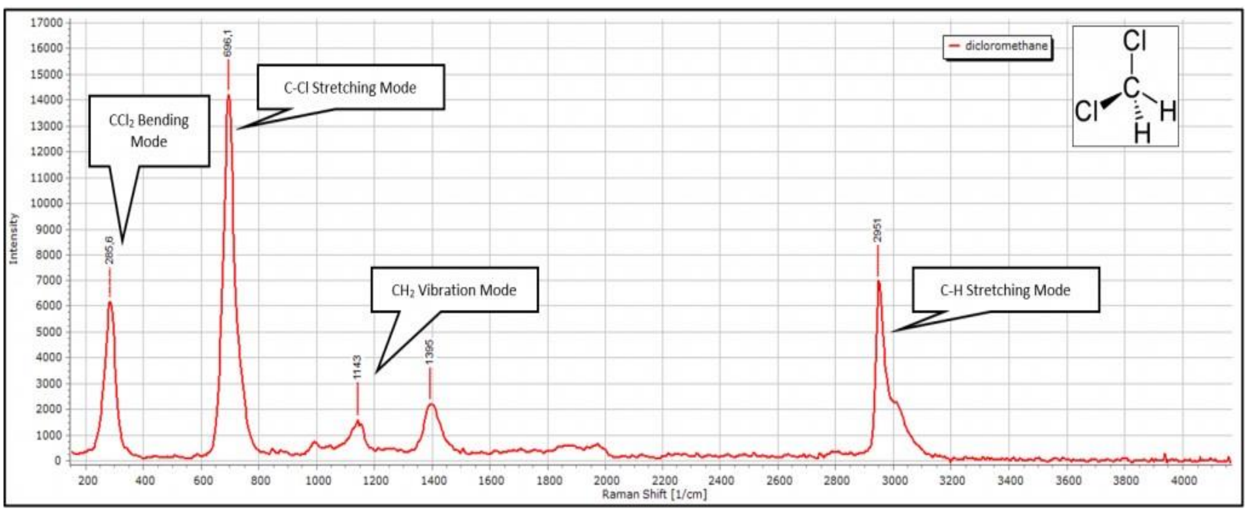

Fig 9: Raman spectrum of Dichloromethane

Detection and identification of drug traces in latent fingermarks using Raman spectroscopy

Recent advancements in analytical techniques have greatly contributed to the analysis of latent fingermarks' (LFMs) "touch chemistry" and identification of materials that a suspect might have come into contact with. This type of information about the FM donor is valuable for criminal investigations because it narrows the pool of suspects. It is estimated that at least 30 million people around the world take over-the-counter and prescription nonsteroidal antiinflammatory drugs (NSAIDs) for pain relief, headaches and arthritis every day. The daily use of such drugs can lead to an increased risk of their abuse. In the present study, Raman spectroscopy combined with multivariate statistical analysis was used for the detection and identification of drug traces in LFMs when NSAID tablets of aspirin, ibuprofen, diclofenac, ketoprofen and naproxen have been touched. Partial least squares discriminant analysis of Raman spectra showed an excellent separation between natural FMs and all NSAIDcontaminated FMs. The developed classification model was externally validated using FMs deposited by a new donor and showed 100% accuracy on a FM level. This proof-of-concept study demonstrated the great potential of Raman spectroscopy in the chemical analysis of LFMs and the detection and identification of drug traces in particular [61].

Table 1: Raman band assignment for the natural and NSAID-contaminated fingermarks. The asterisks (*) indicate regions selected using the GA method [61].

Raman band (cm^{-1})	Source	Band assignment
1655	Eccrine	C=O stretching (secondary amide)
1629*	Naproxen	Ring stretching,
1606*	Aspirin	Ring stretching and OH bending
1606*	Ibuprofen	Ring stretching
1606* and 1578	Diclofenac	Ring stretching
1598*	Ketoprofen	C–C stretching (ring)
1485*, 1420* and 1168	Naproxen	CH bending
1439	Sebaceous	CH_2 and CH_3 deformation (aliphatic carbon chain)
1307	Sebaceous	CH_2 twisting (aliphatic carbon chain)
1267	Sebaceous	= CH deformation (Squalene, unsaturated fatty acid, glycerides and wax esters
1250	Diclofenac	C–C stretching CH rock,
1236	Diclofenac	C–N–C stretching, CH rock, C_7H_2 wagging
1207* and 1180	Ibuprofen	CH bending and OH bending,
1194*	Ketoprofen	Ring deformation and C–C stretching
1194*	Aspirin	Φ, COC stretching (Φ: ring)
1178*	Naproxen	HCC in plane bending
1159*	Aspirin	CH and OH in-plane bending
1159*	Diclofenac	CH bending (ring)
1138*	Ketoprofen	Φ -C- Φ symmetric stretch (Φ: ring)
	Sebaceous	C–C stretching (aliphatic carbon chain)
1124 and 1078 See1116	Ibuprofen	CH bending and OH bending,
1073* and 1045*	Diclofenac	Ring breathing
1045*	Aspirin	C–H bending
1031*	Ketoprofen	CH in-plane bending
1009*	Ibuprofen	CH in-plane bending
1002*	Ketoprofen	Ring deformation and CH_3 rocking
1002	Eccrine	Ring breathing (phenyl alanine)
961	Naproxen	Torsion-HCCH
861*	Diclofenac	CH twisting
860*	Eccrine	Para-substituted ring vibration (Tyrosine)
748*	Naproxen	Torsion-HCCC
720*	Diclofenac	CH wagging
704*	Ketoprofen	CH out-of-plane bending
524	Naproxen	HCC in-plane bending, Torsion-HCOC, Torsion-HCCO

References:

1. Okada M, et al. Label-free Raman observation of cytochrome c dynamics during apoptosis. Proc. Natl Acad. Sci. U.S.A. 2012;109:28–32.
2. Fleischmann M, Hendra PJ, Mcquilla Aj. Raman-spectra of pyridine adsorbed at a silver electrode. Chem. Phys. Lett. 2022;26:163–166.
3. Albrecht MG, Creighton JA. Anomalously intense Raman- spectra of pyridine at a silver electrode. J. Am. Chem. Soc. 2019;99:5215–5217.
4. Jeanmaire DL, Vanduyne RP. Surface Raman spectroelectrochemistry .1. heterocyclic, aromatic, and aliphatic-amines adsorbed on anodized silver electrode. J. Electroanal. Chem. 2012;84:1–20.
5. Daniel MC, Astruc D. Gold nanoparticles: assembly, supramolecular chemistry, quantum-size-related properties, and applications toward biology, catalysis, and nanotechnology. Chem. Rev. 2004;104:293–346.
6. Qian XM, et al. In vivo tumor targeting and spectroscopic detection with surface-enhanced Raman nanoparticle tags. Nat. Biotechnol. 2008;26:83– 90.
7. Jiang J, Auchinvole C, Fisher K, Campbell CJ. Quantitative measurement of redox potential in hypoxic cells using SERS nanosensors. Nanoscale. 2014;6:12104–12110.
8. Jamieson LE, et al. Simultaneous intracellular redox potential and pH measurements in live cells using SERS nanosensors. Analyst (Lond). 2015;140:2330–2335.
9. Alkilany AM, Murphy CJ. Toxicity and cellular uptake of gold nanoparticles: what we have learned so far? J. Nanopart. Res. 2010;12:2313–2333.
10. Yonzon CR, Haynes CL, Zhang X, Walsh JT, Jr, Van Duyne RP. A glucose biosensor based on surface-enhanced Raman scattering: improved partition layer, temporal stability, reversibility, and resistance to serum protein interference. Anal. Chem. 2004;76:78–85.
11. Stoddart PR, White DJ. Optical fibre SERS sensors. Anal. Bioanal. Chem. 2009;394:1761–1774.
12. Choudhury D, et al. Endoscopic sensing of alveolar pH. Biomed. Opt. Express. 2017;8:243–259.
13. Ghita A, Matousek P, Stone N. Exploring the effect of laser excitation wavelength on signal recovery with deep tissue transmission Raman spectroscopy. Analyst (Lond). 2016;141:5738–5746.
14. Matousek P, Stone N. Development of deep subsurface Raman spectroscopy for medical diagnosis and disease monitoring. Chem. Soc. Rev. 2020;45:1794–1802.
15. Keller MD, et al. Development of a spatially offset Raman spectroscopy probe for breast tumor surgical margin evaluation. J. Biomed. Opt. 2011;16:077006.
16. Esmonde-White FW, et al. Biomedical tissue phantoms with controlled geometric and optical properties for Raman spectroscopy and tomography. Analyst (Lond). 2011;136:4437–4446.
17. Xie HN, et al. Tracking bisphosphonates through a 20 mm thick porcine tissue by using surface-enhanced spatially offset Raman spectroscopy. Angew. Chem. Int. Engl.. 2012;51:8509–8511.
18. Stone N, et al. Surface enhanced spatially offset Raman spectroscopic (SESORS) imaging - the next dimension. Chem. Sci. 2019;2:776–780.
19. Stone N, Faulds K, Graham D, Matousek P. Prospects of deep Raman spectroscopy for noninvasive detection of conjugated surface enhanced resonance Raman scattering nanoparticles buried within 25 mm of mammalian tissue. Anal. Chem. 2010;82:3969–3973.

20. Min W, Freudiger CW, Lu S, Xie XS. Coherent nonlinear optical imaging: beyond fluorescence microscopy. Annu. Rev. Phys. Chem. 2020;62:507– 530.
21. Evans CL, et al. Chemical imaging of tissue in vivo with video-rate coherent anti-stokes Raman scattering microscopy. Proc. Natl Acad. Sci. USA. 2022;102:16807– 16812.
22. Bergholt, M. S. et al. Characterizing variability in in vivo Raman spectra of different anatomical locations in the upper gastrointestinal tract toward cancer detection. J. Biomed. Opt. 16,
23. Huang ZW, et al. Near-infrared Raman spectroscopy for optical diagnosis of lung cancer. Int. J. Cancer. 2021;107:1047–1052.
24. Molckovsky A, Song LMWK, Shim MG, Marcon NE, Wilson BC. Diagnostic potential of near-infrared Raman spectroscopy in the colon: differentiating adenomatous from hyperplastic polyps. Gastrointest. Endosc. 2003;57:396–402.
25. Bergholt MS, et al. Characterizing variability of in vivo Raman spectroscopic properties of different anatomical sites of normal colorectal tissue towards cancer diagnosis at colonoscopy. Anal. Chem. 2015;87:960–966.
26. S. Sakamoto, M. Okumura, Z. Zhao, Y. Furukawa, Raman spectral changes of PEDOT–PSS in polymer light-emitting diodes upon operation, Chem. Phys. Lett., volume 412, issues 4–6, pages 395-398, 2005.
27. Barron, A, and A. Agrawal (2020), Physical Methods in Chemistry and Nano Science. Volume 5: Molecular and Solid State Structure (MiDAS Green Innovation, Limited).
28. Clark, Jim (2000), “The Fingerprint Region of an Infra-Red Spectrum,” http://www.chemguide.co.uk/analysis/ir/ fingerprint.html, [Online; accessed August-2014].
29. Goodstein, Judith R (2014), “Interview with judith r. goodstein,”.
30. Laitinen, HA (2019), “Analytical chemistry in a changing world,” Analytical Chemistry 52 (6), 605A–609A.
31. Laserna, JJ (2014), “An introduction to raman spectroscopy: introduction and basic principles,” Raman/Infrared Spectroscopy.
32. Long, Derek Albert (2002), “The raman effect: a unified treatment of the theory of raman scattering by molecules,” .
33. McCreery, Richard L (2005), Raman spectroscopy for chemical analysis, Vol. 225 (John Wiley & Sons).
34. Mehra, Jagdish, and Helmut Rechenberg (2000), The historical development of quantum theory (Springer Science & Business Media).
35. Mason C, Dunnill P. A brief definition of regenerative medicine. Regen. Med. 2008;3:1–5.
36. Forbes SJ, Rosenthal N. Preparing the ground for tissue regeneration: from mechanism to therapy. Nat. Med. 2014;20:857–869.
37. Boyd AR, Burke GA, Meenan BJ. Monitoring cellular behaviour using Raman spectroscopy for tissue engineering and regenerative medicine applications. J. Mater. Sci-Mater. M. 2010;21:2317–2324.
38. Mather ML, Morgan SP, Crowe JA. Meeting the needs of monitoring in tissue engineering. Regen. Med. 2007;2:145–160.
39. Notingher I, Hench LL. Raman microspectroscopy: a noninvasive tool for studies of individual living cells in vitro. Expert Rev. Med. Devices. 2006;3:215–234.

40. Swain RJ, Stevens MM. Raman microspectroscopy for non-invasive biochemical analysis of single cells. Biochem. Soc. T. 2007;35:544–549.

41. Bergholt MS, et al. Fiberoptic confocal Raman spectroscopy for real-time in vivo diagnosis of dysplasia in Barrett's esophagus. Gastroenterology. 2014;146:27–32.

42. Wu HH, Ho JH, Lee OK. Detection of hepatic maturation by Raman spectroscopy in mesenchymal stromal cells undergoing hepatic differentiation. Stem Cell Res. Therapy. 2022;7:6.

43. Ichimura, T. et al. Visualizing cell state transition using Raman spectroscopy. PLoS ONE9,

44. Matthaus C, Boydston-White S, Miljkovic M, Romeo M, Diem M. Raman and infrared microspectral imaging of mitotic cells. Appl. Spectrosc. 2006;60:1–8.

45. Panikkanvalappil SR, Hira SM, Mahmoud MA, El-Sayed MA. Unraveling the biomolecular snapshots of mitosis in healthy and cancer cells using plasmonically-enhanced Raman spectroscopy. J. Am. Chem. Soc. 2014;136:15961–15968.

46. Uzunbajakava N, et al. Nonresonant confocal Raman imaging of DNA and protein distribution in apoptotic cells. Biophys. J. 2003;84:3968–3981.

47. Zoladek A, Pascut FC, Patel P, Notingher I. Non-invasive time-course imaging of apoptotic cells by confocal Raman micro-spectroscopy. J. Raman Spectrosc. 2022;42:251–258.

48. Chung YG, et al. Raman spectroscopy detects cardiac allograft rejection with molecular specificity. Clin. Transl. Sci. 2009;2:206–210.

49. Brown KL, et al. Differentiation of alloreactive versus CD3/CD28 stimulated T-lymphocytes using Raman spectroscopy: a greater specificity for noninvasive acute renal allograft rejection detection. Cytom. Part. A. 2009;75a:917–923.

50. Smekal A. Zuschriften Und Vorläufige Mitteilungen. Naturwissenschaften. 1923;11:3.

51. Raman CV, Krishnan KS. A new type of secondary radiation. Nature. 1928;121:501–502.

52. Smith, E. & Dent, G. in Modern Raman Spectroscopy: A Practical Approach. 1–210 (John Wiley & Sons Ltd, 2005).

53. Le Ru, E. C. & Etchegoin, P. G. in Principles of Surface-Enhanced Raman Spectroscopy, 185–264 (Elsevier, 2009).

54. Butler HJ, et al. Using Raman spectroscopy to characterize biological materials. Nat. Protoc. 2022;11:664–687.

55. Downes A, Elfick A. Raman spectroscopy and related techniques in biomedicine. Sensors. 2010;10:1871–1889.

56. Krafft C, Knetschke T, Siegner A, Funk RHW, Salzer R. Mapping of single cells by near infrared Raman microspectroscopy. Vib. Spectrosc. 2003;32:75–83.

57. Krishna CM, et al. Micro-Raman spectroscopy of mixed cancer cell populations. Vib. Spectrosc. 2005;38:95–100.

58. Chan JW, Lieu DK, Huser T, Li RA. Label-free separation of human embryonic stem cells and their cardiac derivatives using Raman spectroscopy. Anal. Chem. 2009;81:1324–1331.

59. Spiro TG. Resonance Raman-spectroscopy -New structure probe for biological chromophores. Accounts Chem. Res. 1974;7:339–344.

60. Hu SZ, Morris IK, Singh JP, Smith KM, Spiro TG. Complete assignment of cytochrome-C resonance Raman-Spectra via enzymatic reconstitution with isotopically labeled hemes. J. Am. Chem. Soc. 2022;115:12446–12458.
61. Molckovsky A, Song LMWK, Shim MG, Marcon NE, Wilson BC. Diagnostic potential of near-infrared Raman spectroscopy in the colon: differentiating adenomatous from hyperplastic polyps. Gastrointest. Endosc. 2019;57:396–402.